AIMS Geosciences, 8(1): 33–51.
DOI: 10.3934/geosci.2022003
Received: 17 October 2021
Revised: 06 January 2022
Accepted: 10 January 2022
Published: 14 January 2022

http://www.aimspress.com/journal/geosciences

Research article

Can synoptic patterns influence the track and formation of tropical cyclones in the Mozambique Channel?

Chibuike Chiedozie Ibebuchi*

Institute of Geography and Geology, University of Würzburg, Am Hubland, 97074 Würzburg, Germany

*** Correspondence:** Email: chibuike.ibebuchi@uni-wuerzburg.de.

Abstract: The influence of large-scale circulation patterns on the track and formation of tropical cyclones (TCs) in the Mozambique Channel is investigated in this paper. The output of the hourly classification of circulation types (CTs), in Africa, south of the equator, using rotated principal component analysis on the T-mode matrix (variable is time series and observation is grid points) of sea level pressure (SLP) from ERA5 reanalysis from 2010 to 2019 was used to investigate the time development of the CTs at a sub-daily scale. The result showed that at specific seasons, certain CTs are dominant so that their features overlap with other CTs. CTs with synoptic features, such as enhanced precipitable water and cyclonic activity in the Mozambique Channel that can be favorable for the development of TC in the Channel were noted. The 2019 TC season in the Mozambique Channel characterized by TC Idai in March and TC Kenneth afterward in April were used in evaluating how the CTs designated to have TC characteristics played role in the formation and track of the TCs towards their maximum intensity. The results were discussed and it generally showed that large-scale circulation patterns can influence the formation and track of the TCs in the Mozambique Channel especially through (i) variations in the position and strength of the anticyclonic circulation at the western branch of the Mascarene high; (ii) modulation of wind speed and wind direction; hence influencing convergence in the Channel; (iii) and modulation of the intensity of cyclonic activity in the Channel that can influence large-scale convection.

Keywords: circulation type; tropical cyclones; hourly classification; Mozambique Channel; Africa south of the equator

1. Introduction

Ref [1] suggested that the modes of variability in a large-scale circulation can be represented by individual circulation types (CTs), and these modes can influence the formation and track of tropical cyclones (TCs) over the tropical western North Pacific. Thus it is worthwhile to investigate how synoptic patterns in Africa, south of the equator, might influence TC activity in the Mozambique Channel, which experiences intense TC seasons endangering lives and properties especially in Madagascar [2].

The most application of synoptic climatological classifications has been focused on its usage to explain the variability of surface variables [3]. However, it should be equally considered that the large-scale variability of cyclonic and anti-cyclonic systems, which the circulation typing tends to characterize in terms of map types, form the basic dynamics through which the large-scale circulations influence surface variables.

Tropical cyclones (TC) are low-pressure systems intensely rotating cyclonically that form over the tropical oceans [4,5]. They are recurring phenomena in the southwestern Indian Ocean [6]. Based on the maximum wind speed sustained, in the southern hemisphere, they can be characterized as tropical storms, depressions, or cyclones. However, for simplicity, tropical cyclones will be used in this work to cover intense cyclonic systems in the Mozambique Channel. The usual periods for the occurrence of TC, in the Southern Hemisphere, are during peak austral summer and austral autumn seasons (i.e., December–March). This is because these periods are usually characterized by higher sea surface temperature (SST), unstable atmosphere necessary for moist convection, and lower tropospheric vertical shear. The lag, at which TC occurs, amidst the period of maximum insolation, is due to the high heat capacity of ocean waters, which causes them to take several weeks to reach high temperatures. SST is significantly related to the storm intensity [7,8]. Ref [9] noted that an increase in SST by 2 ℃ generally increases the intensity of TCs. Ref [10] explained that the inter-tropical convergence zone (ITCZ), which moves southward in austral summer, brings about the necessary convergence and vorticity for the formation of TC. Ref [10] explained further that in addition to lower SST, strong vertical wind shear and lack of typical ITCZ over the South Atlantic Ocean are reasons why TC is rare at this basin. In the south Indian Ocean, Ref [11] reported that the frequency of TCs that reached category five (i.e. the strongest category of storms) has increased since 1989. Under global warming, at a critical threshold of 2 ℃, the number of TCs making landfall over southern African is projected to decrease [12]. Also, Ref [13] added that under global warming, for the latter part of the 21st century, due to changes in large-scale atmospheric temperature, pressure, and wind profiles of the southern African regions and the adjacent oceans, the preferred landfall position of the TC systems is projected to shift northward over the southern Africa sub-continent.

In the Mozambique Channel, atmospheric conditions are favorable for the development of TCs due to high SST of about 26–28 ℃ in austral summer [14] and weak vertical wind shear [15]. According to Ref [16], values of TC heat potential (i.e. above 40 $kJcm^{-2}$) needed for TC intensification might still be present in the Mozambique Channel up to May. TC within the southwest Indian Ocean occurs on average about three times a year over Madagascar and Mozambique [17]. Most TCs in the Mozambique Channel tracks southeastwards, after approaching Madagascar it recurves into the south Indian Ocean [18]. Also, variability in the strength and position of the Mascarene high influences both the formation and track of TC in the Mozambique Channel [19] especially through the direct influence it has on teleconnections such as the subtropical Indian Ocean

dipole [20] and southeast winds that penetrate the Channel. Repeated tropical cyclogenesis in the Mozambique Channel according to Ref [21] can be attributed to warm SST in the southwest Indian Ocean and anomalous easterly circulations. Ref [22] explained that even though it is less likely that landfall associated with TC will penetrate the interior southern African mainland and the east coast of southern Africa due to the relatively dry interior plateau that covers most of the regions, synoptic conditions coupled with SST anomalies and atmospheric circulations over the Indian Ocean might favor an unusual penetration of TC in the aforementioned regions.

Low-frequency modes of variability at the south Indian Ocean such as the Madden-Julian Oscillation, El Niño Southern Oscillation, and the Indian Ocean Dipole have been noted to influence the frequency of TC occurrence and the spatial pattern of TC in the south Indian Ocean (e.g., [23–25]). Ref [26]noted that when the subtropical Indian Ocean Dipole and the Southern Annular Mode are negative, the formation of TC tends to occur north of the Mozambique Channel and vice versa . Also, Ref [26] noted that the teleconnections especially the Southern Annular Mode and the Madden Julian Oscillation influences perceptible water values. According to Ref [14], the Dipole Mean Index and the Southern Annular Mode coincide with the highest landfall years and also influence the latitudinal and longitudinal track trajectories of TC in the southwest Indian Ocean. Here the focus is on investigating how the synoptic situations characterized by large-scale variability in cyclonic and anti-cyclonic circulations in Africa, south of the equator, influence the track and formation of TCs in the Mozambique Channel.

Ref [27] explained TCs as a little rotating earth on which a complete set of eigenmodes of a dynamic system exist. Ref [28] noted that the combination of sequential and cluster analysis allows for the detection of a TC system up to three days in advance of its start. Applying vector empirical orthogonal function analysis and fuzzy algorithm to obtain recurrent patterns over the tropical western North Pacific Ref [1] concluded that CTs over the basin are related to TC characteristics, revealing their formation and track types. Following the recommendation of Ref [1] on the need for a circulation typing technique that allows overlapping of the classified variables to optimize the physical interpretability of the CTs related to tropical cyclones, this study uses the fuzzy obliquely rotated T-mode principal component analysis (PCA) [29–32] to classify CTs in the study region. The fuzziness of the approach implies that overlapping of the classified variable is allowed so that more than one CTs can be considered at a given realization in line with the continuum nature of atmospheric circulations. The method has been applied successfully in classifying CTs in Africa south of the equator and linking the CTs to rainfall variability and air quality in parts of southern Africa [33–35].

The continuum nature of atmospheric circulation implies also that to understand atmospheric circulation at a given time instant, one needs a clear picture of the previous history of the patterns that occurred. Thus to get the best insight on this issue, using ERA5 reanalysis data set [35] which has SLP, spatially and temporally homogeneous with other fields at an hourly resolution, this study investigates the hourly time development of the CTs and the ability of the CTs examined at a sub-daily scale to explain the track and formation of TCs in the Mozambique Channel using the 2019 TC events of TC Idai and TC Kenneth as reference.

2. Materials and methods

Hourly SLP data set from 2010–2019 and daily SLP data set from 1979–2019 were obtained from ERA5 reanalysis [36] and NCEP-NCAR reanalysis [37] respectively. Both reanalyses data sets were interpolated to a common 2.0 °× 2.0 °longitude and latitude using bilinear interpolation. Ref [38] reported that the reanalysis data sets (ERA-Interim in particular) perform low in producing TCs with a deep pressure center as observed; thus it is acknowledged that the reanalysis data sets might have limitations when used to study TC.

Figure 1 shows the study region for the CT classification (0–50.25 °S; 5.75–55.25 °E). It was chosen to capture the Mozambique Channel; the adjacent ocean to the east coast of Madagascar; the west to east movement of the subtropical high-pressure systems; and the polar fronts—during its northward track. The classification approach of the CTs is the same as applied in previous studies [32–35]. The major difference is that here it is applied also to hourly SLP data.

The classification involves the application of obliquely rotated PCA on the T-mode correlation matrix of the SLP field [29,30]. Singular value decomposition was used to obtain the eigenvalues, PC scores, and eigenvectors. The PC loadings are obtained by multiplying the eigenvectors by the square root of their corresponding eigenvalues, making them responsive to rotation. The PC scores capture the input patterns and the PC loadings localize the input patterns in time [39]. The number of the retained component was based on ensuring that each added component uncovers a unique pattern. The oblique rotation that was made at a power of 2 enhances the physical interpretability of the patterns by removing the orthogonality constraint and maximizing the number of near-zero loadings so that each retained component clusters unique days with similar spatial pattern [29,30]. The absolute value of the loadings reflects an important signal and near-zero loadings weakly contribute to the PC scores [39]. Using a hyperplane threshold of ±0.2, near-zero loadings (noise) are separated from the actual signal [40] so that each component yields clusters of negative and positive loadings above the threshold. To ensure that the patterns are not artifacts of the selected reanalysis data set, choice of the analysis period, and temporal resolution, the daily classification from NCEP was used to validate the sub-daily classification from ERA5 based on the reproduction of the input patterns (PC scores), their eigenvalues and the CTs with their statistics. Furthermore, the classification has not been limited only to the TC season since there are no clear boundaries in the seasonality of CTs so that it will not be accurate to claim that there are summer or winter CTs in the absolute sense, even though a CT might have a high tendency to dominate in a given season. In reality, a CT dominant in summer might still (in rare conditions) occur in winter and vice versa; the idea of seasons is equally imprecise. Thus it might be an advantage to use the complete data set in the circulation typing, and then further analyze the annual cycle of the CTs to isolate the CTs that tend to be dominant at a given season.

The Mozambique Channel is among the basins where TC can develop. A study by Ref [26] analyzed the atmospheric conditions during TC events in the Mozambique Channel using SST, precipitable water, and vertical wind shear. Here, variations in the position and intensity of SLP in the Channel as presented by the classified CTs, together with the composites of precipitable water, wind vector at 850 hPa, and relative vorticity at 850 hPa were used in isolating major CTs with TC characteristics in the basin. The 2019 TC season in the southwest Indian Ocean characterized by two significant cyclonic events in the Mozambique Channel (i.e., the TC Idai and TC Kenneth) were used as reference periods in examining if the CTs designated to characterize conditions under which a TC

might develop in the Channel, played some role during the TC events. In each case, hourly variations in SLP in 4 days were examined based on investigating the CTs assigned to the hours of these days by the classification scheme. The 4 days is a lag of two days before the TC reached its first maximum intensity (as reported and documented by concerned meteorological agency monitoring TC in the basin); the day the TC reached its first maximum intensity; and the following day. After the occurrence/persistence of the CTs with TC characteristics was checked for the 24 hours in each day, the mean of SLP and wind vector at 850 hPa in each of the days are computed, and field correlation was done between the mean SLP of the day and the mean SLP field representing the CT with TC characteristics. A higher correlation suggests that the signal of the CT was more significant on that day, irrespective of the continuum/overlapping nature of the CTs. Furthermore, the relationship between the temporal evolution of the amplitude of the selected CTs and the track and intensity of the TCs are examined. The overreaching goal of the analysis is to check if the time development presented by the sub-daily occurrence of the CTs validates that the CTs designated to possess TC characteristics in the basin, occurred/persisted and have contributed to the formation and track of the TC system.

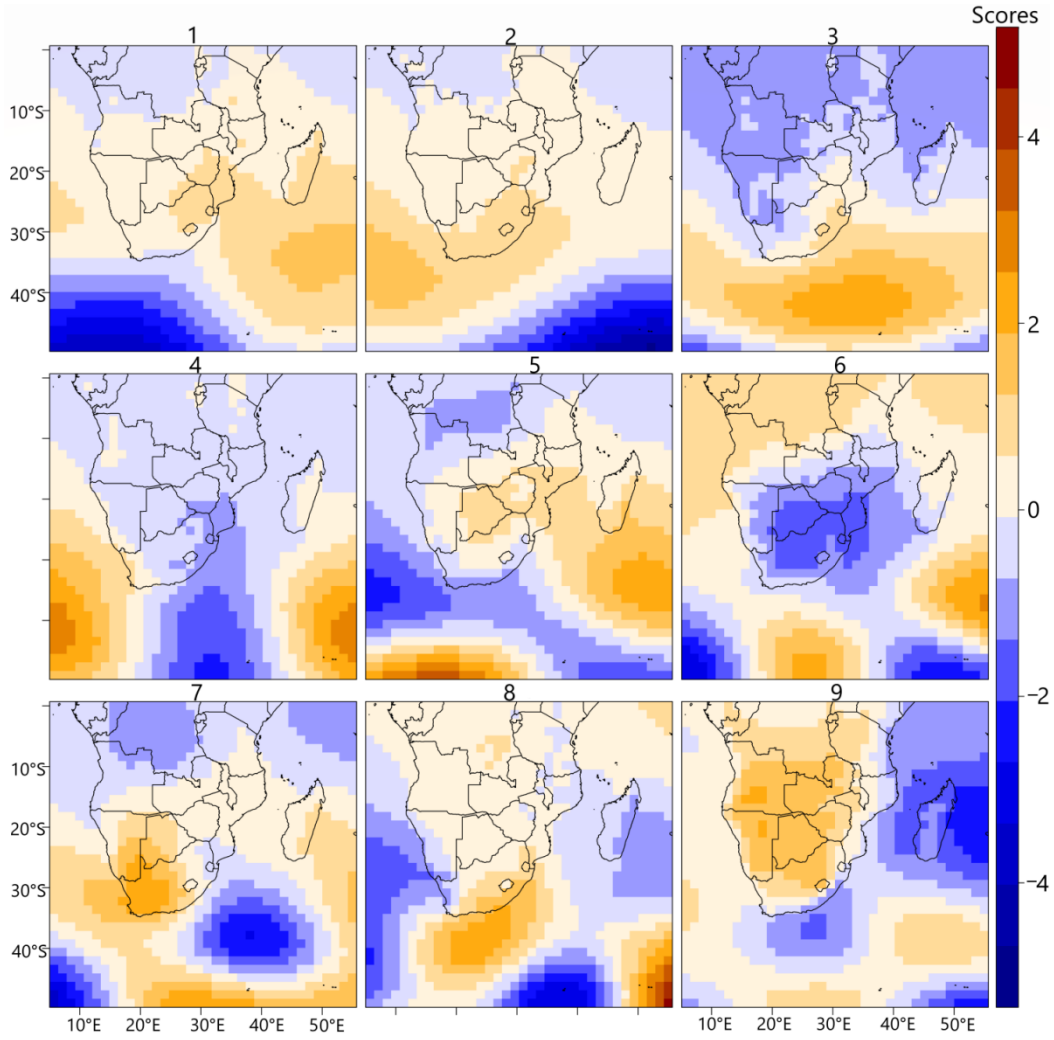

Figure 1. Input patterns (PC scores) from ERA5 hourly classification.

3. Results

3.1. Validation of the hourly CTs from ERA5

Figure 1 shows the input patterns from the 9 retained components as classified from hourly ERA5 SLP data. The congruence coefficients from Table 1 between the patterns from hourly ERA5 classifications and the daily classification using NCEP-NCAR SLP data shows a one to one correspondence and good match (i.e., congruence coefficients are mostly greater than 0.95) indicating that the input patterns presented by the scores, were well reproduced in each case. A possible reason why some patterns have a congruence match below 0.95 can be because, from the hourly data, there could be intra-day variations of the SLP field, due to the atmospheric tide, which might affect the pattern classification and statistics (i.e., compared to the daily classifications). The CTs are designated by the mean SLP field of the clusters in a given class (Figure2).

Table 1. Congruence coefficients between PC scores from ERA5 hourly classification and corresponding PC scores from NCEP-NCAR daily classification.

Score	Congruence coefficient
1	0.99
2	0.99
3	0.99
4	0.99
5	0.96
6	0.95
7	0.98
8	0.93
9	0.93

Figure 3 shows the relative frequency of occurrence of the CTs from the hourly classification in ERA5 and the daily classification from NCEP-NCAR. It can be seen that regardless of the choice of the reanalysis product, temporal resolution, and classification period, the relative frequency of occurrence of the CTs shows satisfactory stability. 1+, 2+, 3+, and 4+ have a relatively higher probability to occur. They can be understood as the dominant states of the atmosphere based on their persistence for a longer time. 1+ is the most frequent and climatology of atmospheric circulation in the region. The annual occurrence of the CTs (e.g., [3,33]) indicated that 1+ is dominant in austral winter, whereas 3+ is specifically the austral summer climatology since it is the most frequent austral summer pattern. 2+ dominates almost in all seasons and 4+ also is dominant in austral summer.

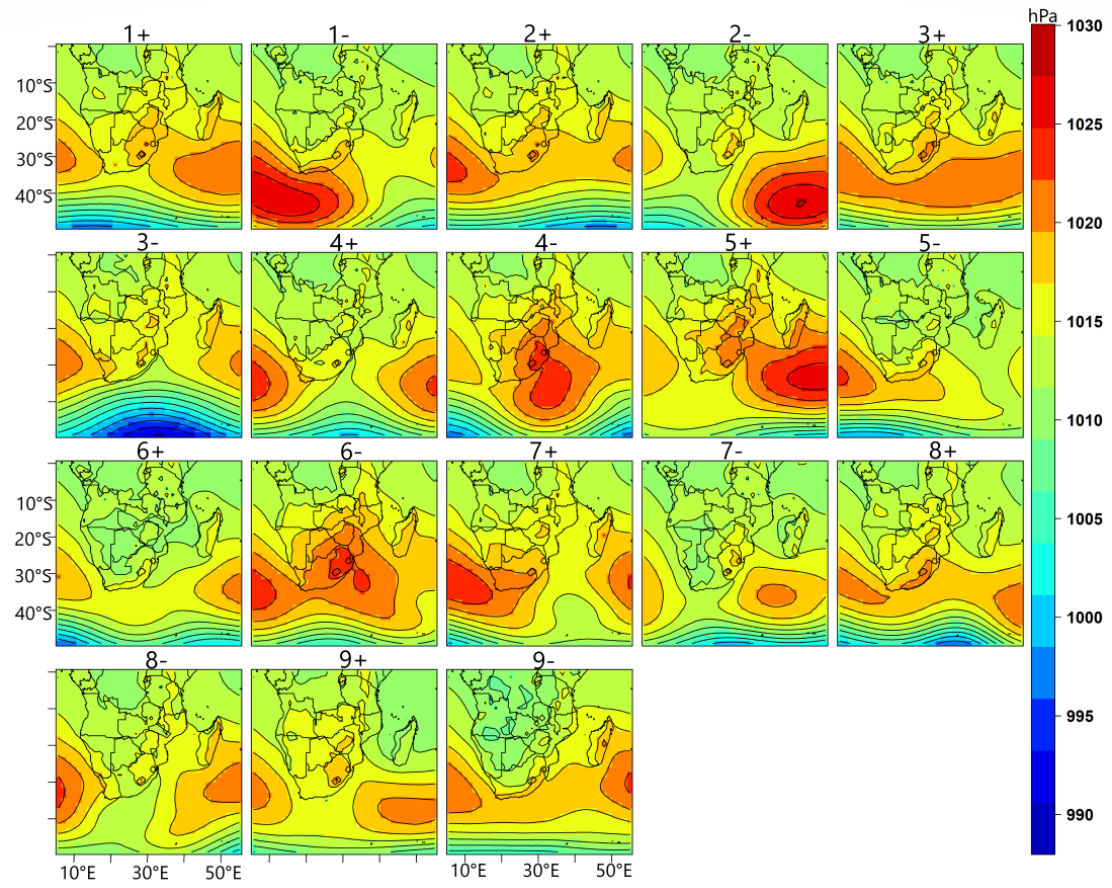

Figure 2. Circulation types in the study region from the ERA5 hourly classification**.**

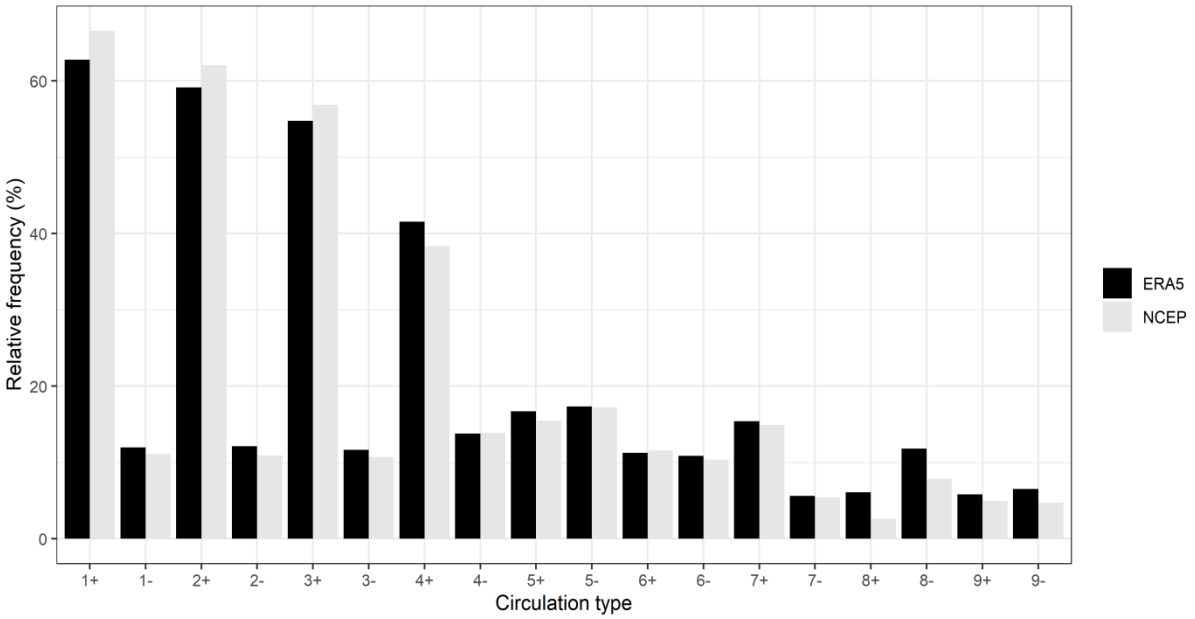

Figure 3. Comparison of the relative frequency of occurrence of the CTs from ERA5 hourly classifications and their counterparts from NCEP-NCAR daily classification.

The input patterns of type 3 and type 4 (Figure 1) indicate two major scenarios of variability in the semi-permanent high-pressure systems during austral summer. Type 3 (i.e., 3+ in this case) shows the west to east movement of the semi-permanent high, which ridges through the Agulhas current towards eastern South Africa. Type 4 (i.e., 4+ in this case) shows a scenario where the western portion of the Mascarene high weakens and the mid-latitude disturbances track further north, allowing the cyclonic system from the Mozambique Channel to move further southwest since atmospheric blocking by the western branch of the Mascarene high is weakened.

3.2. Selections of CTs with tropical cyclone characteristics

TC in the southern hemisphere is usual in austral summer and early austral autumn. Considering the high heat capacity of ocean water, the SST threshold (about 26–28 ℃) necessary for the development of TC can be slowly attained, resulting in why early austral autumn might be the period favorable for TC development in the Mozambique Channel.

From the input patterns in Figure 1, type 9 clearly shows a strong negative anomaly in the Mozambique Channel, apparently blocked by a positive anomaly positioning at the western branch of the Mascarene high. From Figure 2 (i.e., 9+) a strong cyclonic anomaly subjected to atmospheric blocking by the Mascarene high is evident. Based on the composites from precipitable water (PW), wind vector at 850 hPa (Figure 4); relative vorticity, and SST anomaly (not shown), 9+ is the major CT that presents a synoptic state favorable for TC in the Mozambique Channel. According to Ref [15], during TC season in the Mozambique Channel, lower level winds are westerly at about 15 ℃S northward. This is evident in 9+ from Figure 4; since the strong cyclonic anomaly adjusts the cross-equatorial easterly winds to become predominantly westerly towards the northern part of the Channel. Concerning the strong correlation between SST, SLP, and PW and also that the transfer of energy that strengthens the radial circulation within a TC mainly comes through the evaporation of water into the atmosphere, PW is an important field in the monitoring and prediction of the intensity and track of TC. Figure 4 shows that for 9+ PW is relatively enhanced in the Channel and at the east coast of Madagascar. An enhancement of PW implies a drop in SLP and an increase in SST. At the upper levels, PW is equally related to the mass of clouds. Thus PW can be sufficient to approximate an atmospheric condition under which TC might develop. From Figure 5, the annual occurrence of 9+ dominates from February to April, which corresponds to the TC season in the Southern Hemisphere.

6+ is another CT selected to have TC characteristics though with a lesser intensity of the low-pressure system in the Mozambique Channel compared to 9+, and also with a different track altogether. Its input pattern from Figure 1 shows a strong anomaly at the southern landmasses, extending eastward into the southwest Indian Ocean. Unlike in 9+, the western branch of the Mascarene high is weakened allowing the cyclonic system to progress further southwest towards the Agulhas current. Its dominating period from Figure 6 is in the peak of austral summer when continental heating is highest; suggesting that diabatic heating might play a role in generating the positive SST anomalies in the southwest Indian Ocean. It is equally evident that under 6+ cross-equatorial easterly winds are well expressed, transporting moisture from the tropical Indian Ocean into the Channel. PW under 6+ extends also southwest, following the weakening of the western branch of the Mascarene high.

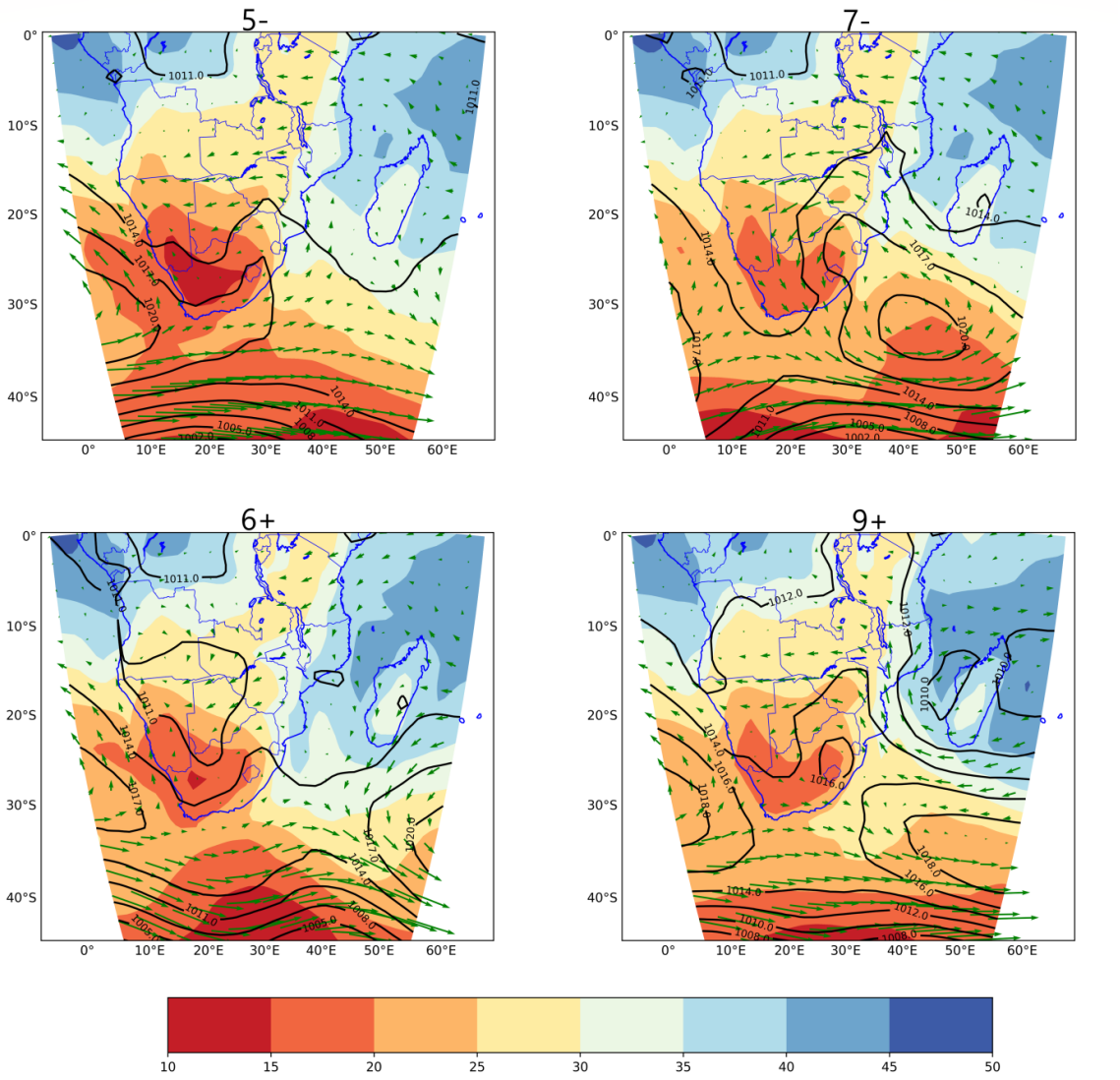

Figure 4. Composite maps for the selected CTs with TC characteristics. The contour line is SLP in hPa. Vector is the wind at 850 hPa in ms^{-1}. Color is precipitable water in kg/m^2.

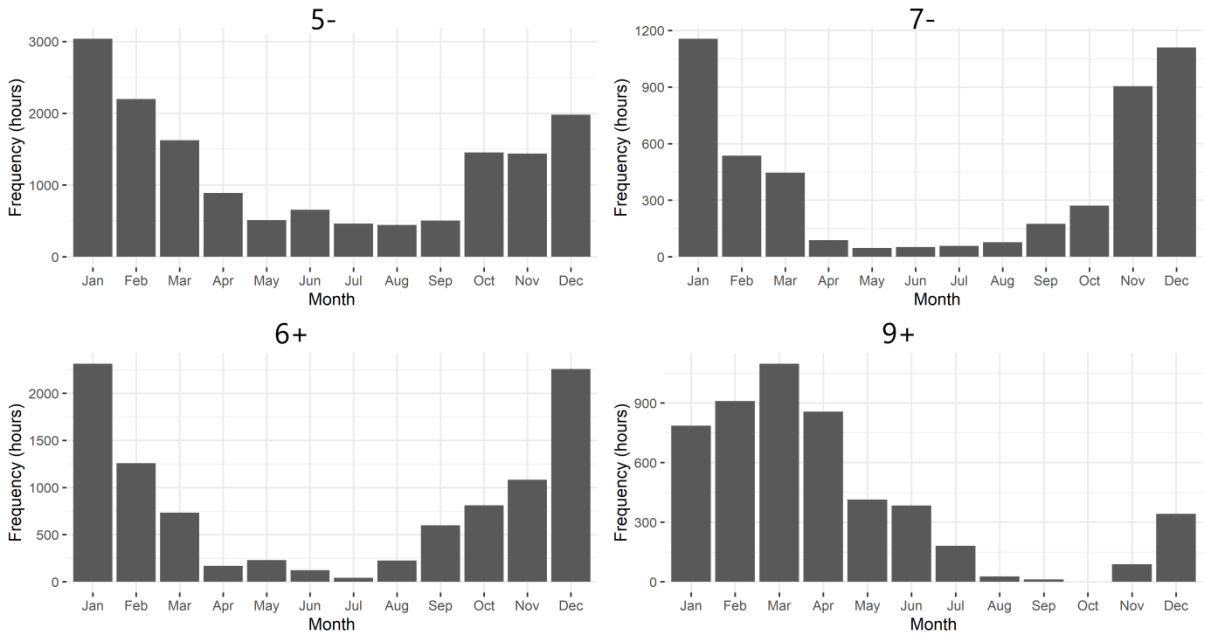

Figure 5. Annual frequency of occurrence of the CTs with TC characteristics from ERA5 hourly classification.

3+ and 4+ though not explicitly selected as TC types should be noted. Since they are austral summer mean patterns, their persistence for a longer time, relative to the winter dominant CTs is crucial in creating the long-term atmospheric condition under which TC might develop in the Channel. Moreover, the persistence of their signal will aid in enhancing the TC characteristics of the CTs designated to have TC features, whereas the occurrence of winter dominant CTs such as 4− and 6−, associated with the dominance of high-pressure system over the southwest Indian Ocean might have a buffering effect on the tropical cyclonic characteristics of the TC types—related to drier air which can inhibit moist convection.

5− presents a synoptic state similar to 6+, concerning a weak state of the western branch of the Mascarene high, thus allowing warm SST in the southwest Indian Ocean. However, Figure 5 shows that PW is higher north of Madagascar (under 5−) suggesting that TC might develop mainly towards the north of the Mozambique Channel under this synoptic state. 7− is also similar to 9+ in terms of the strength of the anticyclonic circulation in the south Indian Ocean high pressure, though the circulation appears relatively stronger under this synoptic state, with the cyclonic system in the Mozambique Channel being weaker. The strong easterly wind associated with a stronger south Indian Ocean high-pressure might aid in steering tropical cyclones towards southern Africa. However, as shown in the case of 9+ (Figure 5), should the intensity of the cyclone in the Mozambique Channel be high, easterly trade winds might be adjusted to westerly rather than steering the cyclonic system to move westward. Hence the mean wind in the Channel will decide if the TC can be steered by either the southeast or northeast trade winds. Moreover, the convergence of the easterly winds in the Channel can influence the storm development through the vorticity it induces. To this end, 9+ and 6+ are the major CTs with synoptic states favorable for the development of TC in the Mozambique Channel, whereas 3+ and 4+ are vital to creating the long-term atmospheric conditions for both the development of the TC and the occurrence of the TC types, whereas 5− and 7− might play vital roles in the development of TC north of the Channel and in its track. Generally, 9+, 7− and 3+ commonly

enhance blocking of the cyclone from moving further south. Conversely, 6+, 5− and 4+ feature the weakening of blocking by the Mascarene high, allowing the TC to move further south. Correlation analysis between the CTs and teleconnection indices such as the Nino3.4 index, SAM index, IOD index, and the SIOD index revealed that teleconnections can modulate the occurrence of the CTs over time (e.g., [32–34]).

3.3. 2019 TC season in the Mozambique Channel and influence of the selected TC types

In this section, it will be investigated if the hourly occurrence of CTs, according to the classification output, influences the time development and track of TCs in the Mozambique Channel. For this purpose, the 2019 TC events of TC Idai and TC Kenneth were analyzed. In each case, the hourly occurrence of the CTs for two days before the TC reached its first maximum intensity, the day the TC reached its first maximum intensity, and a day after the TC reached its first maximum intensity were investigated. Table 2 shows the hourly occurrence of CTs, according to the classification output and for the aforementioned days. It can be seen that the CTs designated as mean patterns (i.e., the most dominant signals) persist for a longer period and overlap with other CTs. Also generally, the hourly occurrence of the CTs reveals that the CTs do not readily change at an hourly scale. It should be noted that a change in pressure pattern (and wind pattern) at a 3 hourly scale is realistic and might be of predictive skill in the direction TC systems will likely travel—TCs will likely move to regions where the pressure drops rapidly. Also, a large drop in pressure ahead of a cyclone might imply that the cyclone is deepening. This is the advantage that a sub-daily analysis of the CTs presents.

Figure 6 shows the mean SLP and 850 hPa vector wind for the selected days, and Table 3 presents the field correlation between the mean SLP patterns of each day and the mean SLP pattern of the selected CTs with TC characteristics. The analyzed days for TC Idai are from 9 March to 12 March. From 9 March to 10 March 19:00 UTC, long persistence of 2+, 3+, 4+, and 5− can be seen (Table 2). Recall that 3+ and 4+ are austral summer mean patterns, and 4+, similar to 5−, presents a weaker state of the western branch of the Mascarene high. Hence the persistence of the combination of 4+ and 5− might suggest a synoptic state associated with a weaker circulation at the western branch of the Mascarene high. From Figure 7, the amplitude of 5− was at its peak on 9 March—significantly dominating the signal of the other CTs. The resultant effect was evident from Figure 6 on 9 March—the semi-permanent high-pressure system appears weakened and relatively more southward, similar to the mean pattern of 5− in Figure 2. A TC can be seen also towards the east coast of northern Mozambique. Recall that 5− favors the development of TC north of the Channel. On 10 March between 20:00 UTC and 21:00 UTC, 7− associated with stronger circulation at the south Indian Ocean high-pressure occurred and this might have contributed to why the Mascarene high moved a bit northward and strengthened. Figure 7 also shows a gradual rise, on 10 March, in the amplitude of 7− and 9+ that favors atmospheric blocking of the TC (and easterly convergence in the Mozambique Channel) even though the signal of 5− still dominates. Following a possible strengthening of convergence by the ITCZ as a result of stronger southeast trade winds penetrating the Mozambique Channel, the TC appears to develop further. Table 3 shows that on 9 March and 10 March, the SLP pattern of 5− tends to be relatively dominant as Figure 7 shows that its signal is strongest during these days. On 11 March 9+ persisted from 7:00 UTC to 9:00 UTC; Table 3 and Figure 7 shows that its pattern and signal, respectively, mostly dominated the others on this day. The SLP and wind vector pattern of 11 March shows equally a strengthening of the south Indian

Ocean high-pressure and convergence of easterly winds (adjusted to westerly) in the Channel. The meteorological history of TC Idai notes that it reached its first peak intensity by 12:00 UTC on 11 March [40]. Also between 21:00 UTC of 11 March and 10:00 UTC, of 12 March, 9+ persisted again so that from Table 3 and Figure 7 its SLP pattern and signal dominates again on 12 March. Furthermore, the mean SLP and wind vector pattern on 12 March shows that the south India Ocean high-pressure strengthened more, further blocking the TC from progressing southward. On the same day (i.e. 12 March) between 5:00 UTC and 10:00 UTC, 6+ occurred together with 9+, but from Table 3, the pattern of 9+ tends to persist more, relatively. It is also remarkable that 4− occurred from 6:00 UTC to 9:00 UTC. 4− is a winter dominant pattern and Figure 2 suggests that through the subsiding motion (enhanced anticyclone) it brings in the southwest Indian Ocean, it might inhibit deep convection in the basin. Its occurrence implies that the TC might further weaken, and from the meteorological history of TC Idai [40,41], it was reported that relative to its strength on 11 March, Idai weakened on the 12 March at the same time (i.e., 6:00 UTC) the classification output noted that 4− started to occur. According to Ref [9]an increase in surface pressure over a TC basin can be related to a decrease in SST and maximum precipitation rate. In a scenario that the classification is solely focused on the TC season, the occurrence of a winter type will not be captured, and this might be a further example of the pitfalls following the oversimplification of synoptic classifications by considering only specific seasons.

Coming to TC Kenneth, on 23 April and 24 April the SLP and wind vector field from Figure 6 shows that the TC was situated north of Madagascar with the Mascarene high northward and strengthened. Given its occurrence period (i.e., during austral autumn when some of the winter dominant CTs are likely to occur), Figure 7 shows that the amplitude of the TC types relatively weakened compared to during the TC Idai season. The classification output showed that 2+ and 3+ which are both associated with the west to east movement of the semi-permanent high-pressure system, ridging through the Agulhas region to eastern South Africa, exceptionally persisted from the onset of 23 April till 21:00 UTC, hence in Figure 7, the signal of 9+ that favors atmospheric blocking was evident (though weak); on 24 April when 6+ co-occurred with them. 6+ persisted for the rest of day till 7:00 UTC of 25 April. From Figure 7, a spike in the amplitude of 6+ is evident on 24 and 25 April. Recall that 6+ implies a weakening of the western branch of the Mascarene high, enabling the TC to progress further southwest. Also, 5− with a similar feature as 6+ persisted for 5 hours on the same day between 9:00 UTC and 13:00 UTC (as can be inferred also from Figure 7). 8−, from Figure 2, that equally supports weakening of semi-permanent high-pressure system, from Table 2 can be seen to have occurred at some points on 25 April. Also between 22.00 UTC and 23:00 UTC, 5− occurred again. Hence Figure 7 shows a spike in the amplitude of the CTs that favor weakening of atmospheric blocking of the TCs from late 23 April to 25 April. The implication of the persistence of the CTs that favors the weakening of the western branch of the Mascarene high is reflected in the mean map for 25 April (Figure 6). Cross equatorial easterly winds are stronger, penetrating further southwest and steering the TC towards the east coast of northern Mozambique. Southeast winds are weakened with the Mascarene high situated further southeast; and cyclonic circulation tends to enhance southwest, towards the Agulhas region. The meteorological history of TC Kenneth reported that it reached its first maximum intensity on 25 April [42]. From Table 3 and Figure 7, the signal of 6+ and 5− dominates on this day. Hence it can be inferred that, unlike TC Idai, the reason why TC Kenneth remained most active at the northern Mozambique Channel during its maximum intensity on 25 April can be partly as a result of the stronger signal of 5−, followed by 6+ which both favors

the buildup of TC towards the north of the Channel, basin-wide warming of the southwest India Ocean and enhancement of the cross-equatorial northeast trade winds steering the TC westward. On 26 April, 5− occurred only at 11:00 UTC, whereas the occurrence of 2+, 3+, and 9+ which are all in favor of stronger west to the east progression of the semi-permanent high-pressure system can counter the warm SST in the southwest Indian Ocean induced from the previous day synoptic states. Also, Figure 7 shows that the amplitude of 9+ that favors atmospheric blocking of the TC dominates on 26 April. Though from Table 3, 26 April, the pattern of 5− dominated, the SLP field of 26 April (Figure 6) clearly shows the low-pressure system located further south away from the Channel, where it will be possibly weakened by the eastward-moving high-pressure systems.

Table 2. Hourly occurrence of the CTs from the classification output for the selected days of the 2019 TC season of TC Idai and TC Kenneth.

Time (UTC)	9 March	10 March	11 March	12 March	23April	24 April	25 April	26 April
0:00	1+,3+,4+,5−	2+,3+,4+,5−	2+,3+,4+	2+,3+,9+	1−,2+,3+	2+,3+	1+,3+,6+	1+,3+,4+,
1:00	3+,4+,5−	2+,3+,4+,5−	2+,3+,4+	2+,3+,9+	1−,2+,3+	2+,3+	1+,3+,6+	1+,3+,4+,
2:00	3+,4+,5−	2+,3+,4+,5−	2+,3+,4+	2+,3+,9+	1−,2+,3+	2+,3+	1+,3+,6+	1+,3+,4+,
3:00	3+,4+,5−	2+,3+,4+,5−	2+,3+,4+,7−	2+,3+,9+	2+,3+	2+,3+	1+,3+,4−,6+	1+,3+,4+,
4:00	3+,4+,5−	2+,3+,4+,5−	2+,3+,4+,7−	2+,3+,9+	2+,3+	2+,3+	1+,3+,4−,6+	1+,3+,4+,
5:00	3+,4+,5−	2+,3+,4+,5−	2+,3+,4+,7−	2+,3+,6+,9+	2+,3+	2+,3+	1+,3+,4−,6+	1+,3+,4+,
6:00	3+,4+,5−	2+,3+,4+,5−	2+,3+,4+,7−	2+,3+,4−,6+,+9+	2+,3+	2+,3+	1+,3+,4−,6+	1+,3+,4+,
7:00	2+,3+,4+,5−	2+,3+,4+,5−	2+,3+,4+,7−,9+	2+,3+,4−,6+,+9+	2+,3+	2+,3+	1+,3+,4−,6+	1+,2+,3+,4+,
8:00	2+,3+,4+,5−	2+,3+,4+,5−	2+,3+,4+,7−,9+	2+,3+,4−,6+,+9+	2+,3+	2+,3+	1+,3+	1+,2+,3+,4+,
9:00	2+,3+,4+,5−	2+,3+,4+,5−	2+,3+,4+,7−,9+	3+,4−,6+,+9+	2+,3+	2+,3+	1+,3+,5−	1+,2+,3+,4+,9+
10:00	2+,3+,4+,5−	2+,3+,4+,5−	2+,3+,4+,9+	3+,6+,+9+	2+,3+	2+,3+	1+,3+,5−	1+,2+,3+,4+,9+
11:00	2+,3+,4+,5−	2+,3+,4+,5−	2+,3+,4+	3+,6+	2+,3+	2+,3+	1+,3+,5−	1+,2+,3+,4+,5−
12:00	3+,4+,5−	2+,3+,4+,5−	1+,2+,3+,4+	3+,6+	2+,3+	2+,3+	1+,3+,5−	1+,2+,3+,4+
13:00	3+,4+,5−	2+,3+,4+,5−	2+,3+,4+	3+,6+	2+,3+	2+,3+	1+,3+,5−,8−	1+,2+,3+,4+

Continued on next page

Time (UTC)	9 March	10 March	11 March	12 March	23April	24 April	25 April	26 April
14:00	3+,4+,5–	2+,3+,4+,5–	2+,3+,4+	3+	2+,3+	2+,3+	1+,3+	1+,2+,3+,4+
15:00	3+,4+,5–	2+,3+,4+,5–	2+,3+	3+	2+,3+	1+,2+,3+	1+,3+,8–	1+,2+,3+,4+
16:00	3+,4+,5–	2+,3+,4+,5–	2+,3+	3+	2+,3+	1+,2+,3+	1+,3+,4+,	1+,2+,3+,4+
17:00	3+,4+,5–	2+,3+,4+,5–	2+,3+	1+,2–,3+	2+,3+	1+,2+,3+	1+,3+,4+,	1+,2+,3+,4+
18:00	2+,3+,4+,5–	2+,3+,4+	2+,3+	1+,2–,3+	2+,3+	1+,2+,3+	1+,3+,4+,	1+,2+,3+,4+
19:00	2+,3+,4+,5–	2+,3+,4+,5–	2+,3+	1+,2–,3+	2+,3+	1+,2+,3+	1+,3+,4+,	1+,2+,3+,4+
20:00	2+,3+,4+,5–	2+,3+,4+,5–,7–	2+,3+	1+,2-,3+	2+,3+	1+,2+,3+	1+,3+,4+,	1+,2+,3+,4+
21:00	2+,3+,4+,5–	2+,3+,4+,5–,7–	2+,3+,9+	1+,2–,3+	2+,3+	1+,2+,3+,6+	1+,3+,4+,	2+,3+,4+
22:00	2+,3+,4+,5–	2+,3+,4+,5–	2+,3+,9+	1+,2–,3+	2+,3+	1+,2+,3+,6+	1+,3+,4+,5–	2+,3+,4+
23:00	2+,3+,4+,5–	2+,3+,4+	2+,3+,9+	1+,2–,3+	2+,3+	1+,2+,3+,6+	1+,3+,4+,5–	2+,3+,4+

4. Conclusions

In this study, the relationship between large-scale circulation patterns and storms that form in the Mozambique Channel was investigated. Using circulation typing, CTs were classified in Africa south of the equator and the CTs that have characteristics favoring the development of TC in the Mozambique Channel were noted. The result showed that during austral summer, two CTs that are mean patterns of atmospheric circulation form two scenarios of variability in the strength and location of the western branch of the Mascarene high. The first is characterized by (i) stronger anticyclonic circulation at the western branch of the Mascarene high, ridging into the east coast of South Africa; (ii) and strengthening of the penetration of southeast trade winds in the Mozambique Channel. The other large-scale circulation scenario is associated with (i) weaker and more eastward state of the Mascarene high allowing cyclonic activity to enhance further southwest; (ii) and enhanced cross-equatorial northeast winds. These CTs overlap with the other austral summer CTs, and this suggests that the dominating pattern of circulation at a given time is likely to be due to the persistence of either of the CTs (i.e., the mean patterns) together with other CTs that have similar circulation characteristics with either of the two dominant CTs.

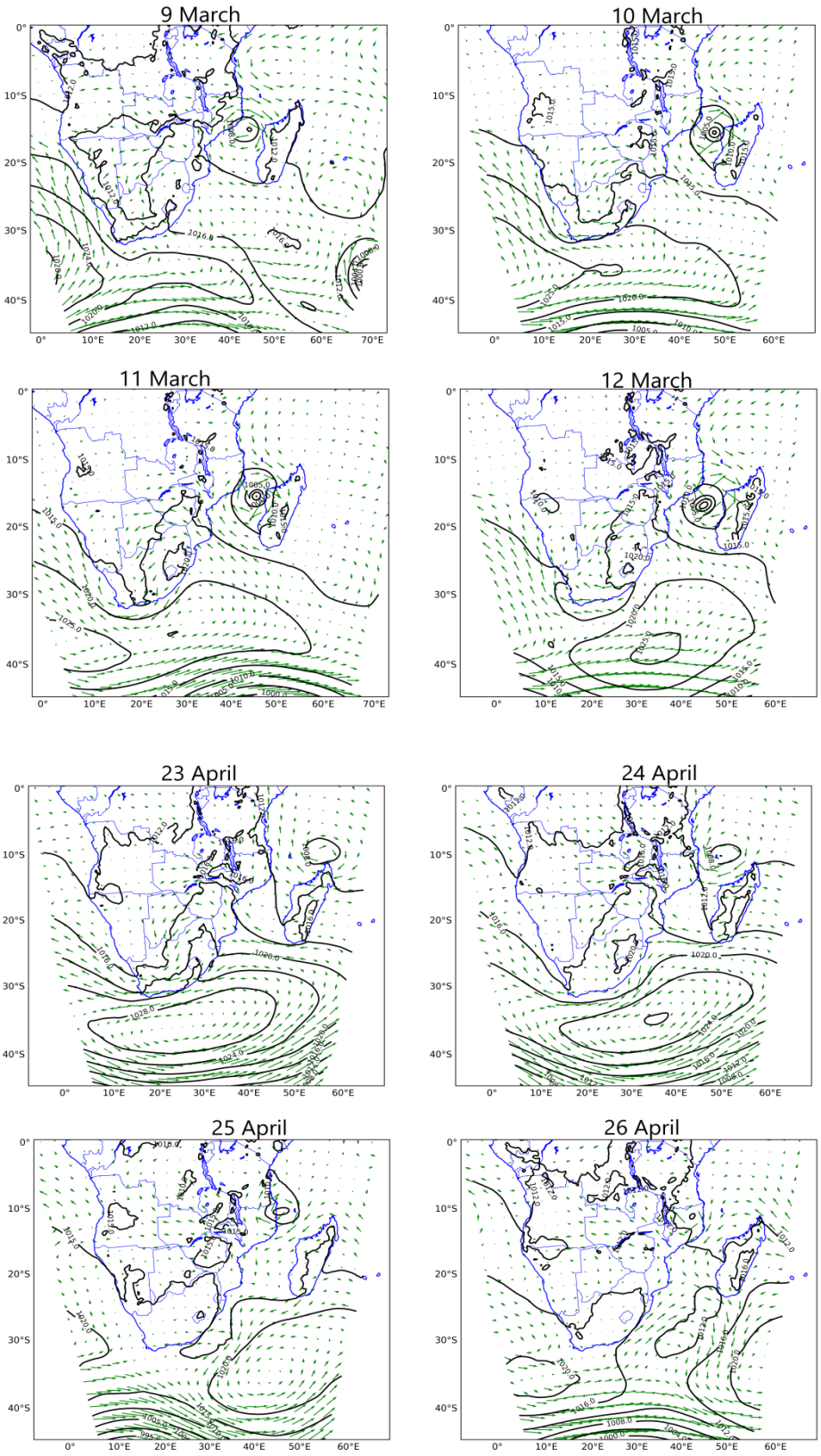

Figure 6. Daily mean SLP and vector wind on selected days during the 2019 TC Idai (top panels) and TC Kenneth (bottom panels) in the Mozambique Channel. Contour is SLP in hPa and the green vector is the wind at 850 hPa in ms^{-1}.

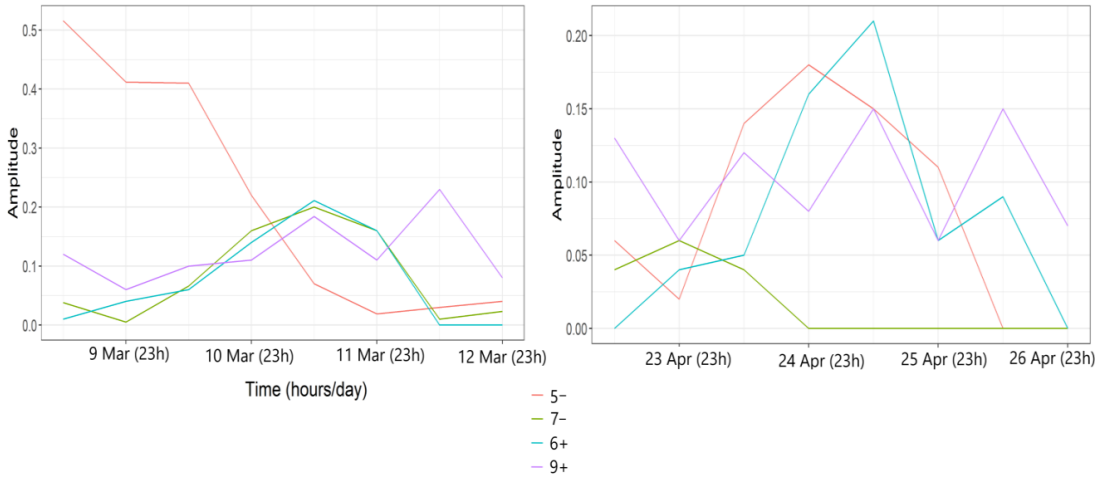

Figure 7. Time evolution in the amplitude of the key CTs that favors TC development in the Mozambique Channel during 9 March to 12 March for the TC Idai (left panel) and from 23 April to 26 April for TC Kenneth (right panel). The amplitude is designated by the mean PC loadings at 12 hourly time frames per day.

During the maximum intensity of cyclone Idai on 11 March, the circulation at the western branch of the Mascarene high was strong and this can be partly attributed to the finding that two days before the TC reached its maximum intensity, there was the domination of the CTs that favor blocking by the Mascarene high. The dominance of the CTs reached its culmination on 11 March. An enhanced circulation at the western branch of the Mascarene high implies that southeasterly winds will further penetrate the Channel favoring convergence with northeast winds. The vorticity and pressure drop induced by the convergence in the Mozambique Channel is likely to have contributed to why TC Idai remained most active in the Mozambique Channel. The synoptic situations during TC Kenneth featured a different scenario: the blocking by the Mascarene high was gradually displaced by the occurrence of CTs favoring the weakening of the western branch of the Mascarene high, and enhancement of northeast winds. The TC which formed north of Madagascar seems to be steered by northeast winds towards northern Mozambique and then southwards away from the Mozambique Channel. For the Mozambique Channel, as a rule of thumb it can be hypothesized that when the western branch of the Mascarene high is most active, a strong TC might be centered at the Mozambique Channel so that Madagascar is mostly at risk since the strong cyclone will equally adjust easterlies (to westerlies) towards Madagascar. On the other hand, when the western branch of the Mascarene high is weakened and more eastward, the TC, which normally develops north of Madagascar, might be driven southwestward by enhanced northerly winds so that the eastern regions of southern Africa—especially Mozambique—might be at risk. Ref [43] reported that during TC Dera, northerly currents steered the TC southward out of the Mozambique Channel.

Acknowledgments

I thank the three anonymous reviewers who helped improve this manuscript.

Data availability

ERA5 datasets are available at https://climate.copernicus.eu/climate-reanalysis. The

NCEP-NCAR reanalysis data is available at https://psl.noaa.gov/data/gridded/data.ncep.reanalysis.html. (accessed on 5 October 2021).

Conflict of interest

The author declares no conflict of interest.

References

1. Harr AP, Elsberry RL (1995) Large-scale circulation variability over the Tropical Western North Pacific. Part 1: spatial patterns and tropical cyclone characteristics. *Mon Weather Rev* 123: 1225–1246. https://doi.org/10.1175/1520-0493(1995)123<1225:LSCVOT>2.0.CO;2
2. Jury MR (1993) A preliminary study of climatological associations and characteristics of tropical cyclones in the SW Indian Ocean. *Meteorl Atmos Phys* 51: 101–115. https://doi.org/10.1007/BF01080882
3. Ibebuchi CC (2021) Circulation pattern controls of wet days and dry days in Free State, South Africa. *Meteorol Atmos Phys* 133: 1469–1480. https://doi.org/10.1007/s00703-021-00822-0
4. Smith RK (2006) Lectures on tropical cyclones. Available from: https://www.meteo.physik.uni-muenchen.de/~roger/Lectures/Tropical_Cyclones/060510_tropical_cyclones.pdf
5. Varotsos CA, Efstathiou MN (2013) Is there any long-term memory effect in the tropical cyclones? *Theor Appl Climatol* 114: 643–650. https://doi.org/10.1007/s00704-013-0875-3
6. Ash KC, Matyas J (2012) The influences of ENSO and the Subtropical Indian Ocean Dipole on tropical cyclone trajectories in the South Indian Ocean. *Int J Climatol* 32: 41–56. https://doi.org/10.1002/joc.2249
7. Pillay MT, Fitchett JM (2019) Tropical cyclone landfalls south of the Tropic of Capricorn, southwest Indian Ocean. *Clim Res* 79: 23–37. https://doi.org/10.3354/cr01575
8. Varotsos CA, Efstathiou MN, Cracknell AP (2015) Sharp rise in hurricane and cyclone count during the last century. *Theor Appl Climatol* 119: 629–638. https://doi.org/10.1007/s00704-014-1136-9
9. Oguejiofor CN, Abiodun BJ (2019) Simulating the influence of sea-surface-temperature (SST) on tropical cyclones over South-West Indian ocean, using the UEMS-WRF regional climate model. *arXiv Atmos Oceanic Phys*.
10. Gray WM (1968) Global view of the origin of tropical disturbances and storms. *Mon Weather Rev* 96: 669–700. https://doi.org/10.1175/1520-0493(1968)096<0669:GVOTOO>2.0.CO;2
11. Fitchett JM (2018) Recent emergence of CAT5 tropical cyclones in the South Indian Ocean. *S Afr J Sci* 114: 1–6. https://doi.org/10.17159/sajs.2018/4426
12. Muthige MS, Malherbe J, Englebrecht FA, et al. (2018) Projected changes in tropical cyclones over the South West Indian Ocean under different extents of global warming. *Environ Res Lett* 13: 065019.
13. Malherbe J, Engelbrecht FA, Landman WA (2013) Projected changes in tropical cyclone climatology and landfall in the Southwest Indian Ocean region under enhanced anthropogenic forcing. *Clim Dyn* 40: 2867–2886. https://doi.org/10.1007/s00382-012-1635-2

14. Pillay MT, Fitchett JM (2020) Southern hemisphere tropical cyclones: A critical analysis of regional characteristics. *Int J Climatol* 41: 146–161. https://doi.org/10.1002/joc.6613
15. Jury MR, Pathack B (1991) A study of climate and weather variability over the tropical Southwest Indian Ocean. *Meteorl Atmos Phys* 47: 37–48. https://doi.org/10.1007/BF01025825
16. Malan N, Reason CJC, Loveday BR (2013) Variability in tropical cyclone heat potential over the Southwest Indian Ocean. *J Geophys Res Oceans* 118: 6734–6746. https://doi.org/10.1002/2013JC008958
17. Malherbe J, Engelbrecht F, Landman W, et al. (2011) High resolution model projections of tropical cyclone landfall over southern Africa under enhanced anthropogenic forcing. South African Society for Atmospheric Sciences 27th Annual Conference, 22–23. http://hdl.handle.net/10204/5680
18. Klinman MG, Reason CJC (2008) On the peculiar storm track of TC Favio during the 2006–2007 Southwest Indian Ocean tropical cyclone season and relationships to ENSO. *Meteorol Atmos Phys* 100: 233–242. https://doi.org/10.1007/s00703-008-0306-7
19. Xulu NG, Chikoore H, Bopape MJM, et al. (2020) Climatology of the Mascarene High and its influence on weather and climate over southern Africa. *Climate* 8: 86. https://doi.org/10.3390/cli8070086
20. Reason CJC (2002) Sensitivity of the southern African circulation to dipole sea-surface temperature patterns in the south Indian Ocean. *Int J Climatol* 22: 377–393. https://doi.org/10.1002/joc.744
21. Chikoore H, Vermeulen JH, Jury MR (2015) Tropical cyclones in the Mozambique Channel: January-March 2012. *Nat Hazards* 77: 2081–2095. https://doi.org/10.1007/s11069-015-1691-0
22. Reason CJC, Keibel A (2004) Tropical cyclone Eline and its unusual penetration and impacts over the southern African mainland. *Weather Forecast* 19: 789–805. https://doi.org/10.1175/1520-0434(2004)019<0789:TCEAIU>2.0.CO;2
23. Gray WM, Sheaffer JD (1991) El Niños and QBO influences on tropical cyclone activity, *Teleconnections linking worldwide climate anomalies*, Cambridge University Press: Cambridge, UK. 535.
24. Varotsos CA (2013) The global signature of the ENSO and SST-like fields. *Theor Appl Climatol* 113: 197–204. https://doi.org/10.1007/s00704-012-0773-0
25. Varotsos CA, Efstathiou MN, Cracknell AP (2013) On the scaling effect in global surface air temperature anomalies. *Atmos Chem Phys* 13: 5243–5253. https://doi.org/10.5194/acp-13-5243-2013
26. Matyas CJ (2015) Tropical cyclone formation and motion in the Mozambique Channel. *Int J Climatol* 3: 375–390. https://doi.org/10.1002/joc.3985
27. Mofor LA, Lu C (2009) Generalized moist potential vorticity and its application in the analysis of atmospheric flows. *Prog Nat Sci* 3: 285–289. https://doi.org/10.1016/j.pnsc.2008.07.009
28. Krapivin VF, Soldatov VY, Varotsos CA, et al. (2012) An adaptive information technology for the operative diagnostics of the tropical cyclones; solar–terrestrial coupling mechanisms. *J Atmos Sol-Tterr Phys* 89: 83–89. https://doi.org/10.1016/j.jastp.2012.08.009
29. Richman MB (1981) Obliquely rotated principal components: an improved meteorological map typing technique? *J Appl Meteoro Climatol* 20: 1145–1159. https://doi.org/10.1175/1520-0450(1981)020<1145:ORPCAI>2.0.CO;2

30. Richman MB (1986) Rotation of principal components. *Int J Climatol* 6: 293–335. https://doi.org/10.1002/joc.3370060305
31. Gong X, Richman MB (1995) On the application of cluster analysis to growing season precipitation data in North America east of the Rockies. *J Clim* 8: 897–931. https://doi.org/10.1175/1520-0442(1995)008<0897:OTAOCA>2.0.CO;2
32. Ibebuchi CC (2021) On the relationship between circulation patterns, the southern annular mode, and rainfall variability in Western Cape. *Atmosphere* 12: 753. https://doi.org/10.3390/atmos12060753
33. Ibebuchi CC (2021) Revisiting the 1992 severe drought episode in South Africa: the role of El Niño in the anomalies of atmospheric circulation types in Africa south of the equator. *Theor Appl Climatol* 146: 723–740. https://doi.org/10.1007/s00704-021-03741-7
34. Ibebuchi CC, Paeth H (2021) The Imprint of the Southern Annular Mode on Black Carbon AOD in the Western Cape Province. *Atmosphere* 12: 1287. https://doi.org/10.3390/atmos12101287
35. Hersbach H, Bell B, Berrisford P, et al. (2020) The ERA5 global reanalysis. *Q J R Meteorol Soc* 146: 1999–2049. https://doi.org/10.1002/qj.3803
36. Kalnay E, Kanamitsu M, Kistler R, et al. (1996) The NCEP/NCAR 40-year reanalysis project. *Bull Am Meteor Soc* 77: 437–472. https://doi.org/10.1175/1520-0477(1996)077<0437:TNYRP>2.0.CO;2
37. Maoyi ML, Abiodun BJ, Prusa JM, et al. (2018) Simulating the characteristics of tropical cyclones over the southwest Indian Ocean using a Stretched-Grid Global Climate Model. *Clim Dyn* 50: 1581–1596. https://doi.org/10.1007/s00382-017-3706-x
38. Compagnucci RH, Richman MB (2008) Can principal component analysis provide atmospheric circulation or teleconnection patterns? *Int J Climatol* 28: 703–726. https://doi.org/10.1002/joc.1574
39. Richman MB, Gong X (1999) Relationships between the definition of the hyperplane width to the fidelity of principal component loadings patterns. *J Clim* 12: 1557–1576. https://doi.org/10.1175/1520-0442(1999)012<1557:RBTDOT>2.0.CO;2
40. Meteo France La Reunion (2019) Tropical Cyclone Idai Warning 12. Available from: http://www.meteo.fr/temps/domtom/La_Reunion/webcmrs9.0/anglais/activiteope/bulletins/cmrs/CMRSA_201903111200_IDAI.pdf
41. Meteo France La Reunion (2019) Tropical Cyclone Idai Warning 15. Available from: http://www.meteo.fr/temps/domtom/La_Reunion/webcmrs9.0/anglais/activiteope/bulletins/cmrs/CMRSA_201903120600_IDAI.pdf
42. Meteo France La Reunion (2019) Intense Tropical Cyclone 14 (Kenneth) Warning 11. Available from: http://www.meteo.fr/temps/domtom/La_Reunion/webcmrs9.0/anglais/activiteope/bulletins/cmrs/CMRSA_201904250600_KENNETH.pdf
43. Reason CJC (2007) Tropical cyclone Dera, the unusual 2000/01 tropical cyclone season in the South West Indian Ocean and associated rainfall anomalies over Southern Africa. *Meteor Atmos Phys* 97: 181–188. https://doi.org/10.1007/s00703-006-0251-2

AIMS Press